Archaeological Prospection
Archaeol. Prospect. **19**, 49–58 (2012)
Published online 18 January 2012 in Wiley Online Library
(wileyonlinelibrary.com) DOI: 10.1002/arp.1417

Short Report

Electrical Resistivity Surveying and Pseudo-Three-Dimensional Tomographic Imaging at Sitio Drago, Bocas del Toro, Panama

THOMAS A. WAKE[1]*, ALEXIS O. MOJICA[2], MICHAEL H. DAVIS[3], CHRISTINA J. CAMPBELL[4] AND TOMAS MENDIZABAL[5]

[1] *Zooarchaeology Laboratory, The Cotsen Institute of Archaeology, University of California, Los Angeles*
[2] *Laboratorio de Ingeniería Aplicada, Centro Experimental de Ingeniería, Universidad Tecnológica de Panamá*
[3] *Department of Anthropology, University of Kansas*
[4] *Department of Anthropology, California State University, Northridge*
[5] *Patronato Panama Viejo, Panama*

ABSTRACT Results of electrical resistivity surveying and pseudo-three-dimensional tomographic imaging at the 15 ha Pre-Hispanic archaeological site of Sitio Drago, Isla Colon, Bocas del Toro province, Panama are presented. The site was occupied between AD 690–1410 and represents the largest known nucleated settlement in the province. A low mound in the centre of the site was selected for intensive electrical surveying in order to locate buried archaeological features. A series of surveys were conducted, including electrical resistivity mapping and pseudo-three-dimensional tomographic imaging. The results revealed a group of resistivity anomalies associated with buried archaeological features. Based on these results, archaeological excavations were targeted that uncovered a cluster of coral slab structures, each containing human remains. Copyright © 2012 John Wiley & Sons, Ltd.

Key words: Geophysical prospection; electrical resistivity mapping; pseudo–three-dimensional tomographic imaging; archaeology; Sitio Drago; Bocas del Toro; Panama

Introduction

Archaeological field research is costly in terms of time, equipment and personnel and sometimes does not produce the desired results. The use of non-invasive geophysical methods can play an important role in focusing archaeological field investigations, as they are both rapid and cost-effective. These methods have been applied to archaeological studies since the 1940s and now constitute an important option for the detection of buried archaeological features. These methods focus on the identification of variation in certain physical properties of buried sediments that can be measured from the ground surface (Linford, 2006). Buried archaeological features that possess physical properties different from the surrounding soil are potentially detectable (Scollar *et al*., 1990; Hesse *et al*., 1997; Stierman and Brady, 1999; Chávez *et al*., 2001, 2005; Bevan and Roosevelt, 2003).

In Panama, recent applications of geophysical prospection to archaeological field studies have focused primarily on Colonial Period sites in central Panama (Caballero *et al*., 2004; Mojica *et al*., 2005, 2007, 2009; Mojica, 2007; Mojica and Garcés, 2008). In order to evaluate their effectiveness at a pre-Columbian site in a different region of Panama, we initiated an electrical prospection programme (resistivity mapping and

* Correspondence to: T. A. Wake, The Cotsen Institute of Archaeology at UCLA, A-210 Fowler Building, 308 Charles E. Young Drive, North, University of California, Los Angeles, California 90095–1510, USA. E-mail: twake@ucla.edu

Received 16 July 2011
Revised 2 November 2011
Accepted 12 December 2011

pseudo-three-dimensional tomographic imaging) at Sitio Drago in Boca del Drago, located in the northwestern corner of Isla Colón in Bocas del Toro province (Figure 1).

Archeological context

The archaeology of Panama covers a long history of terminal Pleistocene colonization, Archaic Period plant domestication, the earliest ceramic production in Central America and subsequent regional diversification and development of complex chiefdoms (Cooke, 2005). However, the archaeology of Bocas del Toro Province and Isla Colón remained completely unknown until 1949, when Matthew Stirling led an expedition to the region (Stirling and Stirling, 1964). This project located and excavated several sites in the Almirante Bay region including one on the beach at Punta Drago. They were unable to locate the larger site now known as Sitio Drago, some 500 m southwest of the point, probably due to the dense foliage covering the beach ridge and flats at the time (Stirling and Stirling, 1964, pp. 275–77). Burton Gordon (1962) undertook the next archaeological investigations in the region and noted a distinct absence of archaeological sites on Isla Colón.

Linares and Ranere (1980) conducted extensive excavations at several shell midden localities on the Aguacate Peninsula at Cerro Brujo. They report that the population of Cerro Brujo and the Aguacate Peninsula numbered no more than 120 persons divided among four hamlets, each consisting of small structures roughly 300 m apart (Linares and Ranere, 1980, p. 66). Five radiocarbon dates illustrate that the Cerro Brujo sites were occupied between AD 880–1250 (Linares, 1977). Linares (1977, p. 311) states that 'the archaeological settlements of Bocas province appear to represent marginal populations organized on the basis of small family (?) groups, without status differentiation or political organization of any recognizable kind.' Linares and Ranere (1980, p. 66) suggest that the populace of the Aguacate Peninsula, and by popular extension, the Bocas del Toro region, existed in a cultural 'backwater'.

Sitio Drago, a much larger (15 ha) site with several low (1–2 m in height) mounds, appears more internally complex than the loosely organized farming hamlets seen at Cerro Brujo, suggesting the presence of a large population and a greater degree of interregional

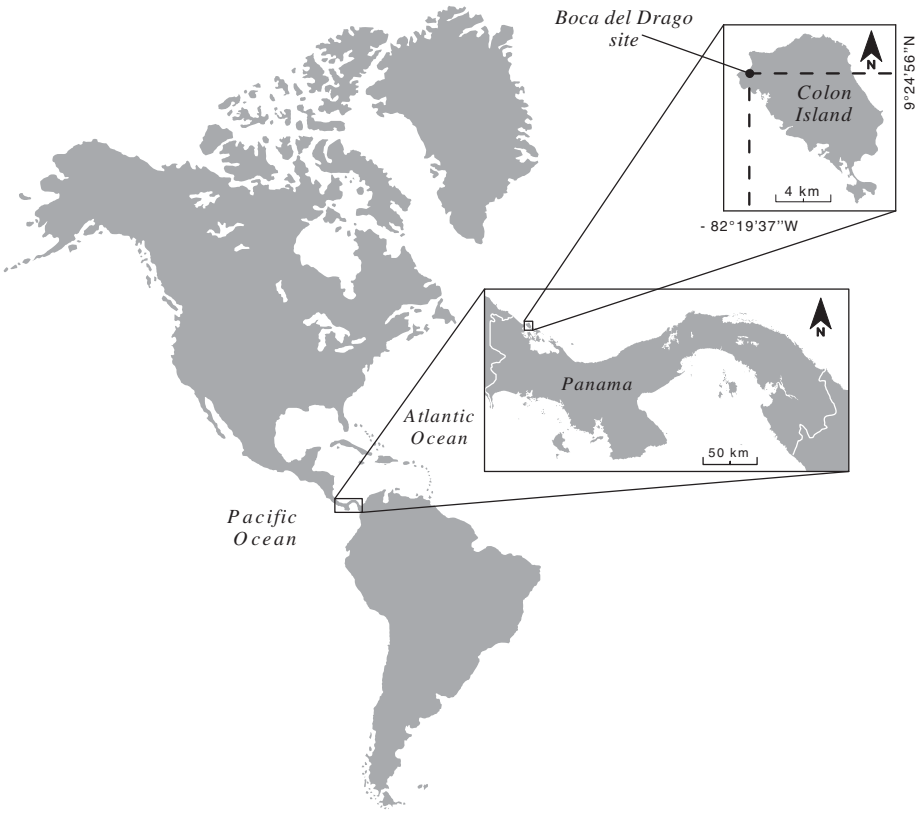

Figure 1. Geographical location of Sitio Drago, Boca del Drago, Colon Island, Bocas del Toro province, Panamá.

DOI: 10.1002/arp

contact. Ceramic evidence recovered to date indicates strong links with the Pacific coastal regions of central Panama (Coclé), western Panama and Costa Rica (Chiriquí and Diquís) and even as far as central and northwestern Costa Rica (Guanacaste). The presence of broken jaguar effigy metates and sculpture fragments from surface contexts and many shell and bone ornaments recovered during excavation hints at the presence of elite goods and possible social ranking (Wake *et al*., 2004).

The presence of basin milling stones, carbonized remains of tree crops, a diverse array of terrestrial forest reptiles and mammals and a variety of reef, mangrove and offshore fish at Sitio Drago generally supports Linares' (1976, 1977; Linares and Ranere, 1980) subsistence model for Cerro Brujo. However, the presence of flat milling stones may suggest that a more mixed seed–root–tree cropping focus operated at Drago as opposed to solely root crops at Cerro Brujo. Fifteen radiometric age determinations date occupation of Sitio Drago to AD 690–1410 (Wake *et al*., 2004; Wake, 2006; Wake and Mendizábal, in press), contemporaneous with Cerro Brujo.

Geologic context of the island and description of the study area

As an island in the Bocas del Toro Archipelago, Isla Colon is geologically part of the Bocas del Toro Basin and includes extensive Neogene sequences extending from the early Miocene to the early Pleistocene (Coates *et al*., 2005). The oldest known geological sequences on Isla Colon are estimated at 20 million years and represent a deep tropical marine channel formed well before the rise of the Isthmus of Panama. Igneous and sedimentary rocks, evidence of volcanic activity and erosion that occurred between 16 and 10 million years ago, form the majority of the archipelago's rocky basement complex (Guzmán and Guevara, 1998a, 1998b). In general, the exposed limestone formations of Isla Colon correspond to the late Pliocene.

According to Coates *et al*. (2005), three lithostratigraphic units are present: the Old Bank Formation, the oldest, includes blue-grey mudstones, fine sandstones, fine volcanic conglomerates and interwoven beds of volcanic rock; the La Gruta Formation, covering the north-central part of the Island, consists of extensive deposits of recrystallized reefs and reef rubble, while the southerly part of the formation is primarily limestone; and the Ground Creek Formation, which is comprised of newer reef deposits that are inserted and superimposed within the La Gruta Formation.

Boca del Drago (9°24′56″N, 82°19′37″W) is located on the northwestern corner of Isla Colon, some 18 km to the northwest of the city of Bocas del Toro (Figure 2), and is characterized geologically by Holocene silts and sands. The areas discussed in this study lie near the centre of the 15 ha archaeological site (Figure 3). The site itself lies on top of a stabilized beach ridge consisting of reworked coralline sands derived from reef erosion.

Electrical prospection

The study area is a 1288 m^2 surface polygon (see Figure 2). The sediments in this area are archaeological in nature and include a great deal of organic material, shell, bone and various stone and ceramic artefacts. Based on the results of previous archaeological test excavations, the well-drained nature of the soil and the existence of nearby marshy areas led to the selection of electrical resistivity as the preferred method of geophysical prospection.

The technique that was used in this study involved the injection of an electrical current into the ground through two metal electrodes (A and B) and the measurement of the potential difference by another pair of electrodes (M and N) that were inserted into the ground elsewhere. A 50 V AC flow injection system with a 4.95 mA maximum output was used. The actual resistivity meter used is a prototype, with the circuit board constructed by Nicolas Florsch at Universite du París 6. The resultant voltage measurement is a function of the amount of current injected, the resistivity of the specific soil volume being interrogated, and the position and geometry of the electrodes. Due to the prevailing telluric noise at the site and the desired shallow depth of investigation (1.2 m), a dipole (pole–pole) electrode configuration was selected where the four electrodes are configured as: $AM = a$, and $AN = BM = BN = \infty$. The electrodes A and M were moved in unison between measurement stations and the remaining electrodes (B and N) were placed some distance from the survey area. This configuration has been used in a variety of archaeological applications (Kampke, 1999; Dabas *et al*., 2000; Papadopoulos *et al*., 2005, 2006; Mojica, 2007; Mojica *et al*., 2007; Mojica and Garcés, 2008).

Electrical resistivity mapping

To obtain information regarding lateral variation of apparent resistivity in the area of interest, electrical resistivity surveying was conducted in groups of parallel transects with an orientation of 88° east of true north. Each transect was placed 0.50 m apart across

DOI: 10.1002/arp

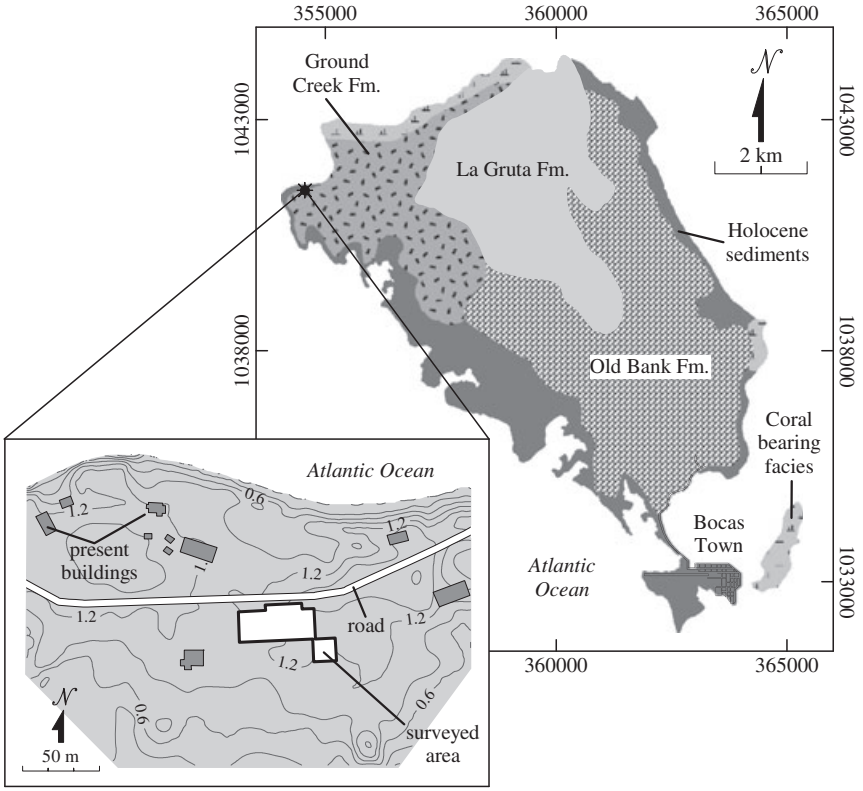

Figure 2. Generalized geological map of Isla Colon (Coates *et al*., 2005) and topographic map (Wake *et al*., 2004) showing the study area at Sitio Drago, Isla Colon, Bocas del Toro, Panama.

Figure 3. Panoramic photograph of the study area, Sitio Drago, Boca del Drago.

the entire surface of the survey area, as illustrated in Figure 4. Apparent resistivity values were recorded every 0.50 m along a given profile. Electrodes A and M were spaced 0.50 m apart. A schematic representation of the distribution of these transects across the study area is depicted in Figure 4a. Figure 4b shows the mobile device used in this study.

In total, 5387 measurements were interpolated using the minimum curvature method (Smith and Wessel, 1990). Figure 5 illustrates the variation in apparent resistivity and the location of the archaeological excavations both before and after the surveying.

A large group of electrical anomalies were interpreted to a depth of approximately 0.50 m. The colour map in Figure 5 clearly illustrates a strong anomaly of high apparent resistivity (> 140 ohm.m in red/black tones) with a northwest–southeast orientation. The highest values of apparent resistivity (> 220 ohm.m) are concentrated on the northern part of this anomaly, near a wire fence and the border of the road; the majority of the anomaly is characterized by values between 140 and 220 ohm.m. The remaining anomalies that are presented in the map (in yellow/green/blue tones) have values that range between 33 and 140 ohm.m. The presence of a few tree

DOI: 10.1002/arp

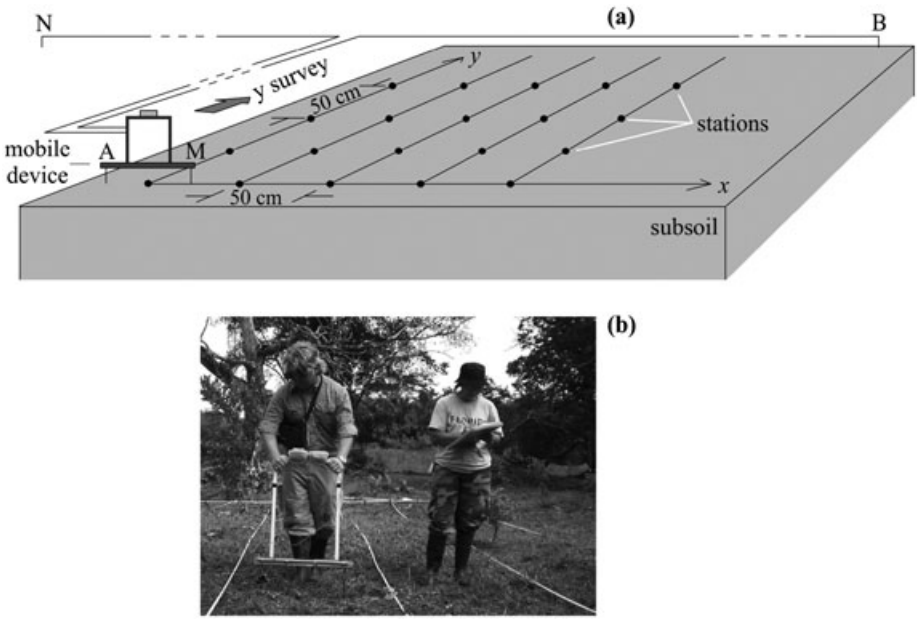

Figure 4. (a) Conventional representation for electrical resistivity mapping (pole–pole array). (b) The mobile device containing electrodes A and M in the field.

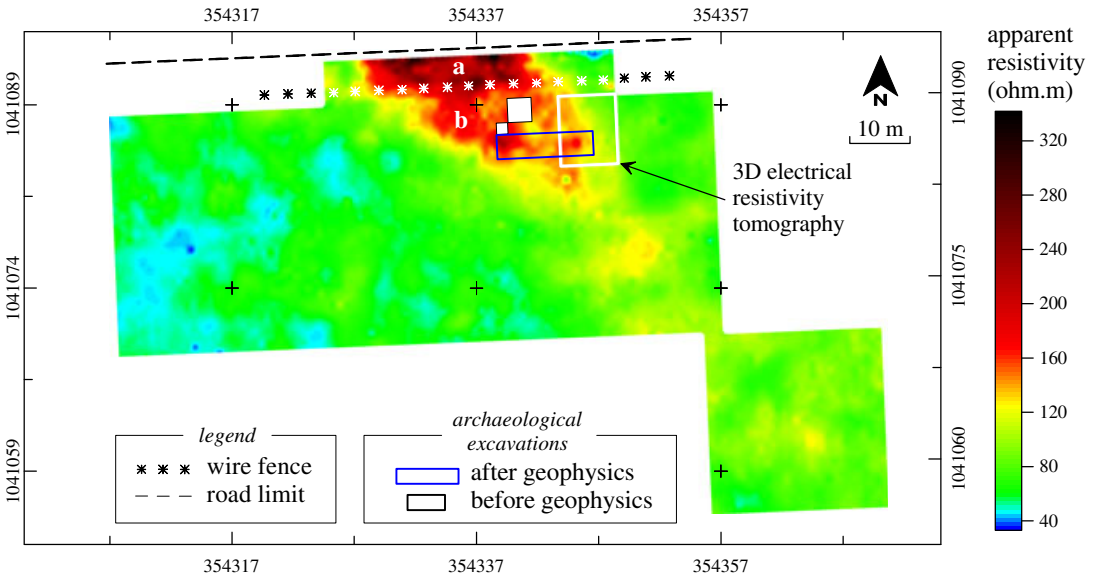

Figure 5. Map of apparent resistivity in the area of interest (pole–pole array, with $a = 0.50$ m), archaeological excavations and other cultural features.

roots in the upper layer of soil did not adversely affect the resistivity readings due to their relatively small size and the close spacing of the electrodes.

Pseudo-three-dimensional tomographic imaging

In order to obtain information about anomalies deeper than 0.50 m a group of 20 parallel transects were placed 0.25 m apart over a length of 5.75 m, covering an area of 30 m^2 within the survey area, as represented by the white rectangle in Figure 5. The objective of this type of electric prospection is to obtain a pseudo-three-dimensional image of the subsurface resistivity structure.

The values of the apparent resistivity, represented by a d column vector, were generated from the same current source that was used in the electrical resistivity mapping; this source was interconnected to a system that controlled a greater number of electrodes

DOI: 10.1002/arp

(switched and wired) that was located along a single transect with a constant separation. The first value of the group of data d was obtained by measuring the potential difference starting from the first two electrodes A_1 and M_1. For the remaining data, the operation was repeated, separating sequentially in each subsequent measurement the potential electrode M until a proportional maximum distance was achieved to reach the desired depth. Figure 6a depicts a schematic diagram of the distribution of the electrodes and the process of measurement of the apparent resistivity along a single transect. Figure 6b is a picture of the system in the area of interest.

To obtain a pseudo-three-dimensional image of the resistivity structure of this low mound, inverse modelling was performed (see Constable *et al*., 1987; deGroot-Hedlin and Constable, 1990). The objective was to determine a model that matches the apparent resistivity data measured in the uppermost 50 cm surface, d_{me}. The model corresponds to the distribution of electrical resistivity deeper below the ground and constitutes a set of model parameters m. The model response $G(m)$ corresponds to the synthetic resistivity data obtained from the governing equations that define the model of a specific parameter set. To characterize the model's parameters, it is necessary to divide the sample area into a group of rectangular cubic elements or prisms. The electrical resistivity values of these elements will then correspond to the model parameters. This calculation is carried out by solving the following second-order differential equation:

$$-\nabla\left[\frac{1}{\rho(x,y,z)}\nabla V(x,y,z)\right] = I\delta(x_S)\delta(y_S)\delta(z_S) \quad (1)$$

where $\rho(x, y, z)$ is the distribution of the electric resistivity in three-dimensional space, I is the current intensity located in the point (x_S, y_S, z_S), δ corresponds to the delta of the Dirac function and $V(x, y, z)$ is the distribution of the electric potential. The pseudo-three-dimensional modelling algorithm is based on an approach of finite difference using the geometry of a pseudo-three-dimensional mesh developed by Dey and Morrison (1979).

The group of measured data, d_{me}, represents a non-linear function of the model parameters m. The problem is then solved in multiple iterations. In each

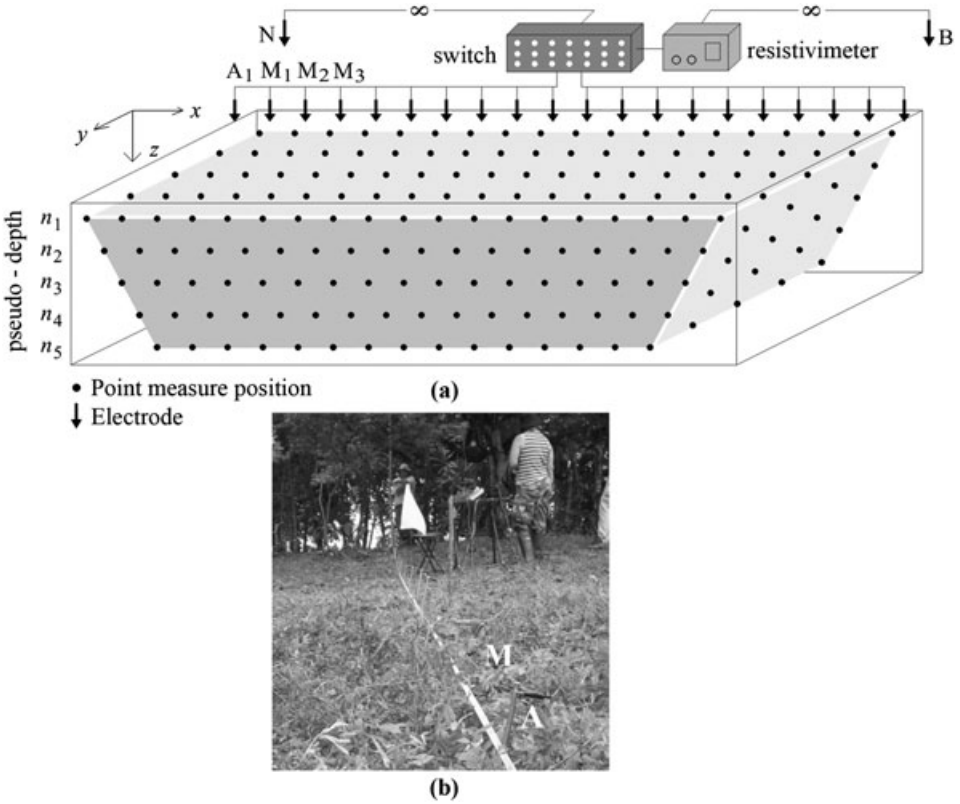

Figure 6. (a) Conventional representation for pseudo-three-dimensional tomographic imaging (pole–pole array) and (b) distribution of the electrodes A and M and rest of the electrodes along a given transect.

DOI: 10.1002/arp

iteration of the inversion a new model, Δm_k is obtained through resolution of the linearized system of the following equations:

$$\Delta \mathrm{m}_k = \left(\mathbf{J}_k^T \mathbf{J}_k + \tau_k \mathbf{W}^T \mathbf{W}\right)^{-1} \mathbf{J}_k^T (\mathbf{d}_{me} - G(\mathrm{m})) - \tau_k \mathbf{W}^T \mathbf{W} \mathrm{m}_{k-1} \quad (2)$$

To obtain the new model at the beginning of the $k+1$ iteration, we applied the equation:

$$\mathrm{m}_{k+1} = \mathrm{m}_k + \Delta \mathrm{m}_k \quad (3)$$

In Equation (2), **W** represents a data weighting matrix, τ is a damping factor and J corresponds to the Jacobian matrix of the model parameters, i.e:

$$\mathbf{J} = \frac{\partial G(m)}{\partial m} \quad (4)$$

Constable *et al.* (1987) and deGroot-Hedlin and Constable (1990) originally described the smoothed model inversion presented in Equation (2). To solve the inverse problem we used the program EarthImager 3D (Advanced Geosciences, Inc.). The result of the inversion is shown in the pseudo-three-dimensional images of Figure 7.

A strong electrical anomaly (resistivity higher than 186 ohm.m (yellow–red) is interpreted between 2.88 and 5.20 m along the x axis, and 1.58 and 4.75 m along the y axis, with a depth range between 0.15 and 0.58 m. The remaining anomalies illustrated in green and blue have electrical resistivity values between 27 and 186 ohm.m.

Discussion

Based on the results of the electrical prospection presented above, an archaeological excavation was conducted to examine the strong anomaly detected in

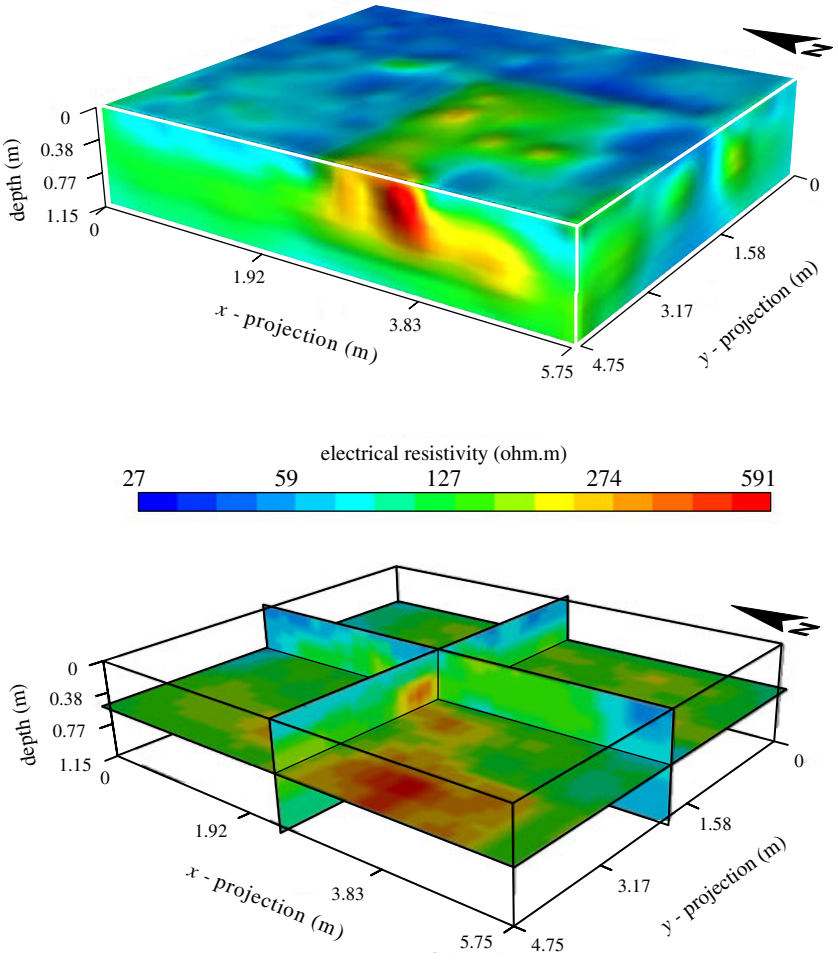

Figure 7. (a) A pseudo-three-dimensional image of the inverted electric resistivity produced by EarthImager 3D. (b) Profiles of the inverted electric resistivity. The green quadrangular area visible on the surface represents the removal of the top 10 cm of soil in the east end of the 2 × 8 m trench, with the exception of a single 1 × 1 m unit (in blue).

DOI: 10.1002/arp

the electrical resistivity survey. Figure 8 presents the visual results of this investigation.

The strong anomaly illustrated in Figure 5 (< 120 apparent resistivity ohm.m) and the anomaly illustrated in the three-dimensional tomographic imaging (Figure 7, < 186 ohm.m) are both associated with archaeological features constructed of coral slabs for the interment of human remains or cist tombs. These tombs generated values and calculated apparent resistivity much higher than the surrounding soil. The remaining lower intensity anomalies are associated with the anthropogenic nature of the material that constitutes the low mound itself: various artefacts and faunal remains in much greater relative densities than the surrounding, slightly lower, areas of the site. All these findings have been corroborated through archaeological excavation.

Figure 8. Result of the archaeological excavation in the area comprising the strong electrical anomaly detected in the mapping of apparent resistivity in Figure 5 and the pseudo-three-dimensional tomographic imaging in Figure 7.

The high apparent resistivity evident at the western end of the 2 × 8 m trench outlined in Figure 5 corresponds to the two parallel elongate cist tombs (Tomb I and Tomb II) visible at the top of the trench in Figure 8. Due to a lack of available stone on Isla Colon (Coates *et al.*, 2005) these tombs are constructed entirely out of flat slabs of elkhorn coral (*Acropora palmata*) taken from the nearby fringing reef. Upon discovery, an overlapping layer of flat coral slabs that had slumped in the middle covered Tombs I and II. These two tombs share a relatively level bottom, with the slabs of each slightly offset. The sides of these tombs consist of one course of large vertical slabs. These tombs contained the skeletal remains of three individuals, Burials 1, 2 and 3. Burials 1 and 2 were extended and facing upward. Burial 1 is complete, with the head to the southeast. Burial 2 was originally complete, with the head to the northwest. The portion of Burial 2 below the pelvis was disturbed by the placement of Burial 3.

Burial 3 was inserted between Tombs I and II through the southeastern portion of Tomb II, disturbing the lower limbs of Burial 2. Burial 3 consists of the remains of a wrapped secondary burial containing one individual. Burial 3 was headless and included parallel upper and lower limb bones that were placed over most of the vertebrae, ribs and selected hand and foot elements.

Tomb III is located roughly in the middle of the 2 × 8 m trench that is illustrated in Figure 8. This feature contained Burial 4, a headless but otherwise complete, extended, upward facing individual with the shoulders to the southeast. While well constructed, Tomb III differs from the first two tombs in that it had vertical slabs along the long sides but not at the ends.

The archaeological feature in the foreground of Figure 8, Tomb IV, represents the anomaly illustrated in Figure 7. The flat, relatively level coral slabs represent capstones found covering Tombs I–III. The visible near-vertical coral slabs represent either the sides and ends of the cist, as seen in Tombs I and II, or perhaps the upturned edges of a concave bottom as seen in Tomb III. As of the publication of this article, Tomb IV remains unexcavated.

Conclusions

The electrical resistivity mapping and tomographic imaging conducted at Sitio Drago have allowed us to visualize the lateral variation of apparent resistivity of the subsoil to a depth of approximately 0.75 m. The ability to visualize electrical anomalies combined

DOI: 10.1002/arp

with excavation has allowed us to associate specific resistivity values with dense archaeological deposits found in certain areas of the site. The pseudo-three-dimensional tomographic imaging resulted not only in more detailed visualization of the lateral variation of soil resistivity, but also the relative depths of electrical anomalies associated with buried cultural features, specifically tombs. The rest of the analyses generated a set of anomalies associated with sedimentary soil containing a high degree of organic material. The site itself includes other areas of interest, including several other low mounds and surface manifestations, so we plan to continue geophysical exploration in order to detect and test other possible buried archaeological features.

Acknowledgements

We would like to thank to the Laboratorio de Ingeniería Aplicada of the Centro Experimental de Ingeniería, Universidad Tecnológica de Panamá and the Cotsen Institute of Archaeology at the University of California, Los Angeles for their continued support of this project. SENACYT, Panamá, provided a generous grant to Mendizabal and Wake supporting the 2007–8 field and laboratory investigations. The American Philosophical Society provided support to the project through a Franklin Research Grant. David and Marvalee Wake have provided continued moral and financial support for the project. Thanks to ITEC and Peter Lahanas for their support early in the project. We thank Helen Campbell, Joanne Snowden, Hans Barnard, Marta Perez and especially Marillyn Holmes for their tireless volunteer efforts. We also thank Doug Doughty, Jerry Howard, Michael Kay and all the students who have participated in the Proyecto Arqueológico Sitio Drago Field Schools. Katie Cramer identified the coral slabs. We thank Brian Damiata for his insightful comments that greatly improved this article. We extend a special thanks to Mrs Ana Serracín de Shaffer, Aristides 'Bolo' Serracín and the entire Serracín family for their permission and encouragement to conduct this project on their land. Finally, any errors or omissions are entirely ours.

References

Bevan BW, Roosevelt AC. 2003. Geophysical explorations of Guajará, a prehistoric earth mound in Brazil. *Geoarchaeology* **18**(3): 287–331.

Caballero O, Mojica AO, Martín-Rincón J. 2004. Prospecciones geofísicas y arqueológicas para la recuperación de la traza urbana de Panamá La Vieja: el caso de la calle Santo Domingo. *Geofísica* **60**: 22–43.

Chávez RE, Cámara ME, Tejero A, Barba L, Manzanilla L. 2001. Site characterization by geophysical methods in the archaeological zone of Teotihuacan, Mexico. *Journal of Archaeological Science* **28**: 1265–1276.

Chávez RE, Cámara ME, Ponce R, Argote D. 2005. Use of geophysical methods in urban archaeological prospection: the Basilica de Nuestra Señora de La Salud, Patzcuaro, Mexico. *Geoarchaeology* **20**(5): 505–519.

Coates AG, McNeill DF, Aubry MP, Berggren WA, Collins LS. 2005. An introduction to the geology of the Bocas del Toro Archipelago, Panama. *Caribbean Journal of Science* **41**(3): 374–391.

Constable S, Parker RL, Constable CG. 1987. Occam's inversion: A practical algorithm for generating smooth models from electromagnetic sounding data. *Geophysics* **52**(3): 289–300.

Cooke RG. 2005. Prehistory of Native Americans on the Central American Land Bridge: colonization, dispersal, and divergence. *Journal of Archaeological Research* **13**(2): 129–187.

Dabas M, Hess A, Tabbagh J. 2000. Experimental resistivity survey at Wroxeter archaeological site with fast and light recording device. *Archaeological Prospection* **7**(2): 107–118.

DeGroot-Hedlin C, Constable S. 1990. Occam's inversion to generate smooth, two-dimensional models from magnetotelluric data. *Geophysics* **55**(12): 1613–1624.

Dey A, Morrison HF. 1979. Resistivity modeling for arbitrarily shaped three-dimensional structures. *Geophysics* **44**(4): 753–780.

Gordon BL. 1962. Notes on shell mounds near the Caribbean coast of Western Panama. *Panama Archaeologist* **5**.

Guzmán HM, Guevara CA. 1998a. Arrecifes coralinos de Bocas del Toro, Panamá: I. Distribución, estructura y estado de conservación de los arrecifes continentales de la Laguna de Chiriquí y la Bahía Almirante. *Revista de Biologia Tropical* **46**(3): 601–623.

Guzmán HM, Guevara CA. 1998b. Arrecifes coralinos de Bocas del Toro, Panamá: II. Distribución, estructura y estado de conservación de los arrecifes de las Islas Bastimentos, Solarte, Carenero y Colón. *Revista de Biologia Tropical* **46**(4): 889–912.

Hesse A, Barba L, Link K, Ortiz A. 1997. A magnetic and electrical study of archaeological structures at Loma Alta, Michoacan, Mexico. *Archaeological Prospection* **4**: 53–67.

Kampke A. 1999. Focused imaging of electrical resistivity data in archaeological prospecting. *Journal of Applied Geophysics* **41**: 215–227.

Linares OF. 1976. 'Garden hunting' in the American tropics. *Human Ecology* **4**(4): 331–349.

Linares OF. 1977. Adaptive strategies in Western Panama. *World Archaeology* **8**(3): 304–319.

Linares OF, Ranere AJ. (eds). 1980. *Adaptive Radiations in Prehistoric Panama*. Peabody Museum Monographs, No. 5. Harvard University: Cambridge.

Linford N. 2006. The application of geophysical methods to archaeological prospection. *Reports on Progress in Physics* **69**: 2205–2257.

Mojica AO. 2007. Application des méthodes géophysiques à la détection des sites précolombiens dans la région centrale de Panama et paramétrisation géoarchéologique dans le site hispanique de Panama Viejo. PhD dissertation, University of Paris 6, France.

Mojica AO, Garcés A. 2008. Electrical prospection applied to detect buried colonial remains at Las Monjas de la

DOI: 10.1002/arp

Concepción Convent, Old Panama archaeological site. *International Journal of South American Archaeology* **3**: 29–35.
Mojica AO, Florsch N, Morón J. 2005. Corrections of archaeological magnetic anomalies of the El Caño pre-columbian site, Panama. *Geofísica* **61**: 59–68.
Mojica AO, Mayo J, Mayo C, Chantada J, De Gracia G, Florsch N. 2007. Resultados de las prospecciones magnética y eléctrica del yacimiento arqueológico El Caño (NA – 20), Gran Coclé, Panamá. *Revista Española de Antropología Americana* **37**(1): 111–126.
Mojica AO, Chichaco E, Navarro M, Pastor L, Vanhoeserlande R. 2009. Magnetic investigation of cultural features in the west zone of the Old Panama archaeological site (Central America). *International Journal of South American Archaeology* **5**: 59–66.
Papadopoulos NG, Sarris A, Kokkinou E, *et al*. 2005. Contribution of multiplexed electrical resistance and magnetic techniques to the archaeological investigations at Poros, Greece. *Archaeological Prospection* **13**(2): 75–90.
Papadopoulos NG, Tsourlos P, Tsokas GN, Sarris A. 2006. Two-dimensional and three-dimensional resistivity imaging in archaeological site investigation. *Archaeological Prospection* **13**(3): 163–181.
Scollar I, Tabbagh A, Hesse A, Herzog I. 1990. *Archaeological Prospecting and Remote Sensing*. Cambridge University Press: Cambridge.
Smith WHF, Wessel P. 1990. Gridding with continuous curvature splines in Tension. *Geophysics* **55**(3): 293–305.
Stierman DJ, Brady JE. 1999. Electrical resistivity mapping of landscape modifications at the Talgua Site, Olancho, Honduras. *Geoarchaeology* **14**(6): 495–510.
Stirling MW, Stirling M. 1964. Archaeological notes on Almirante Bay, Bocas del Toro, Panama. In *Bureau of American Ethnology Bulletin 191*, Anthropological Papers 72. Smithsonian Institution: Washington, DC; 255–284.
Wake TA. 2006. Prehistoric exploitation of the swamp palm (*Raphia taedigera*: Arecaceae) at Sitio Drago, Isla Colón, Bocas Del Toro. *Caribbean Journal of Science* **42**(1): 11–19.
Wake TA, Mendizábal T. In press. Sitio Drago (Isla Colon, Bocas del Toro, Panama): un aldea y centro de intercambio en el Caribe Panameño. In *Mucho Más que un Puente Terrestre: Avances de la Arqueología Panameña y sus Implicaciones en el Contexto Regional*, Martín JG, Cooke RG (eds). Patronato Panamá Viejo: Panamá.
Wake TA, De León J, Fitzgerald C. 2004. Prehistoric Sitio Drago, Bocas del Toro, Panama. *Antiquity* **78**(300). http://antiquity.ac.uk/projgall/wake/index.html

DOI: 10.1002/arp